Long Distance, Bridge-Mediated Electron Transfer in a Ligand-Bridged $Re^{I}-Re^{I}$ Complex

Geoffrey F. Strouse, Jon R. Schoonover,† Richard Duesing,‡ and Thomas J. Meyer*

Department of Chemistry, The University of North Carolina at Chapel Hill, Chapel Hill, North Carolina 27599-3290

Received April 8, 1994®

Laser flash excitation (420 nm) of CH_3CN solutions containing $[(py\text{-}PTZ)(CO)_3Re(\mu\text{-}bbpe)Re(CO)_3(MQ^+)](PF_6)_3$, (py-PTZ is 4-(10-methylphenothiazine)-4′-methyl-2,2′-bipyridine; bbpe is 1,2-*trans*-bis(4′-methyl-2,2′-bipyrid-4-yl)ethene; MQ^+ is N-methyl-4,4′-bipyridinium hexafluorophosphate) results in formation of the redox-separated state $[(py\text{-}PTZ^{\bullet+})(CO)_3Re^{I}(\mu\text{-}bbpe)Re^{I}(CO)_3(MQ^{\bullet})](PF_6)_3$ as shown by transient resonance Raman measurements. It appears during the (~5 ns) laser pulse following $Re^{I} \rightarrow bbpe$, $\pi \rightarrow \pi^*(bbpe)$ excitation and a series of intramolecular electron transfers. The rate constant for back electron transfer is $k(CH_3CN, 298\ K) = 5.56 \times 10^7\ s^{-1}$. Similarly, $Re^{I} \rightarrow bbpe$, $\pi \rightarrow \pi^*(bbpe)$ excitation of $[(py\text{-}PTZ)(CO)_3Re(\mu\text{-}bbpe)Re(CO)_3(py\text{-}PTZ)](PF_6)_2$ leads to $[(py\text{-}PTZ^{\bullet+})(CO)_3Re^{I}(\mu\text{-}bbpe^{\bullet-})Re^{I}(CO)_3(py\text{-}PTZ)](PF_6)_2$ during the laser pulse. It returns to the ground state with $k(CH_3CN, 298\ K) = 2.33 \times 10^7\ s^{-1}$. In the model $[(4\text{-}Etpy)(CO)_3Re(\mu\text{-}bbpe)Re(CO)_3(4\text{-}Etpy)](PF_6)_2$, there is a lowest-lying $\pi-\pi^*$ excited state and a close-lying MLCT state which dominates excited state decay and emission at room temperature. The results of transient absorption measurements suggests that these states coexist at room temperature and undergo relatively slow interconversion.

Introduction

In the study of photoinduced electron transfer, polypyridyl complexes of Ru^{II}, Os^{II}, and Re^{I} have played an important role.[1-5] In appropriately designed chromophore–quencher complexes, metal-to-ligand charge transfer (MLCT) excitation is followed by rapid intramolecular electron transfer to give transient, redox-separated states, e.g.[6]

$$[(bpy)Re^{I}(CO)_3(py\text{-}PTZ)]^+ \xrightarrow{h\nu} [(bpy^{\bullet-})Re^{II}(CO)_3(py\text{-}PTZ)]^+ \rightarrow [(bpy^{\bullet-})Re^{I}(CO)_3(py\text{-}PTZ^{\bullet+})]^+$$

or lower-lying MLCT excited states[7]

$$[(bpy)Re^{I}(CO)_3(MQ^+)]^{2+} \xrightarrow{h\nu} [(bpy^{\bullet-})Re^{II}(CO)_3(MQ^+)]^{2+} \rightarrow [(bpy)Re^{II}(CO)_3(MQ^{\bullet})]^{2+}$$

where bpy is 2,2′-bipyridine, py-PTZ is 10-(4-picolyl)phenothiazine, and MQ^+ is the *N*-4-methyl-4′-bipyridinium cation.

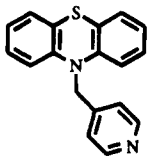

py-PTZ

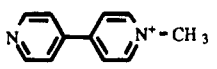

MQ^+

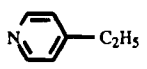

4-Etpy

In molecular assemblies containing both covalently attached donors and acceptors, excitation followed by electron transfer can lead to intramolecular redox separation, e.g.

$$[(PTZ\text{-}bpy)Re^{I}(CO)_3(MQ^+)]^{2+} \xrightarrow{h\nu} [(PTZ\text{-}bpy^{\bullet+})Re^{I}(CO)_3(MQ^{\bullet})]^{2+} \quad (1)$$

where bpy-PTZ is 4-(10-methylphenothiazine)-4′-methyl-2,2′-bipyridine.[8]

One advantage of metal complexes in the study of molecular assemblies is the use of coordination chemistry to create "molecular spacers" between the donor and acceptor by the

† Analytical Chemistry Group, CST-1, Los Alamos National Laboratory, Los Alamos, NM 87544.

‡ This paper is in memory of Dr. Richard Duesing. Rich obtained his Ph.D. in Chemistry from The University of North Carolina at Chapel Hill in 1990 and then took a postdoctoral position at Los Alamos National Laboratory. His tragic death in an automobile accident in November 1991 cut short a promising scientific career.

® Abstract published in *Advance ACS Abstracts,* December 1, 1994.

(1) (a) Juris, A.; Balzani, V.; Barigelletti, F.; Campagna, S.; Belser, P.; Von Zelwesky, A. *Coord. Chem. Rev.* **1988**, *84*, 85. (b) Krause, R. A. *Struct. Bonding (Berlin)* **1987**, *67*, 1. (c) Meyer, T. J. *Pure and Appl. Chem.* **1986**, *58*, 1576. (d) Sutin, N.; Creutz, C. *Pure Appl. Chem.* **1980**, *52*, 2717. (e) Balzani, V.; Scandola, F. *Supramolecular Photochemistry,* Ellis Horwood: Chiehester, **1991.** (f) Meyer, T. J. *Accs. Chem. Res.* **1989**, *22*, 163.

(2) (a) Wang, Y.; Schanze, K. S. *Inorg. Chem.* **1994**, *33*, 1354. (b) Ford, W. E.; Rodgers, M. A. J. *J. Phys. Chem.* **1994**, *98*, 3822. (c) Mecklenburg, S. L.; Peek, B. M.; Erickson, B. W.; Meyer, T. J. *J. Am. Chem. Soc.* **1991**, *113*, 8540.

(3) (a) Leasure, R. M.; Sacksteader, L. A.; Nesselrodt, D.; Reitz, G. A.; Demas, J. N.; Degfraff, B. A. *Inorg. Chem.* **1991**, *30*, 1330. (b) Chen, P. Y.; Duesing, R. D.; Graff, D.; Meyer, T. J. *J. Phys. Chem.* **1991**, *95*, 5850. (c) Creutz, C.; Chou, M.; Netzel, L.; Okumura, M.; Sutin, N. S. *J. Am. Chem. Soc.* **1980**, *102*, 1309. (d) Westmoreland, T. D.; Schanze, K. S.; Neveux, Jr., P. E.; Danielson, E.; Sullivan, B. P.; Chen, P. Y.; Meyer, T. J. *Inorg. Chem.*, **1985**, *24*, 2596.

(4) (a) Lee, E. J.; Wrighton, M. S. *J. Am. Chem. Soc.* **1991**, *113*, 8562. (b) Cooley, L. F.; Larson, S. C.; Elliott. C. M.; Kelly, D. F. *J. Phys. Chem.* **1991**, *95*, 10694. (c) Resch, U.; Fox, M. A. *J. Phys. Chem.* **1991**, *95*, 6169. (d) Haga, M.; Kiyoshi, I.; Boone, S. R.; Pierpont, C. G. *Inorg. Chem.* **1990**, *29*, 3795. (e) Perkins, T. A.; Humer, W.; Netzel, T. L.; Schanze, K. S. *J. Phys. Chem.* **1990**, *94*, 2229.

(5) (a) Ohno, T. Yoshimura, A.; Prasad, D. R.; Hoffman, M. Z. *J. Phys. Chem.* **1991**, *95*, 4723. (b) Ohno, T.; Yoshimura, A.; Mataga, N. *J. Phys. Chem.* **1990**, *94*, 4871. (c) Kitamura, N.; Obati, R.; Kim, H-B.; Tazuke, S. *J. Phys. Chem.* **1989**, *93*, 5764. (d) Navon, G.; Sutin, N. *Inorg. Chem.*. **1974**, *13*, 2159.

(6) (a) Chen, P Y; Westmoreland, T. D.; Danielson, E. D.; Schanze, K. S.; Anthon, D.; Neveaux, P. E.; Meyer, T. J. *Inorg. Chem.* **1987**, *26*, 1116. (b) Chen, P.; Danielson, E.; Meyer, T. J. *J. Phys. Chem.* **188**, *92*, 3708. (c) Chen, P.; Westmoreland, T. D.; Meyer, T. J. Manuscript in preparation.

(7) (a) Chen, P Y; Danielson, E. D.; Meyer, T. J. *J. Phys. Chem.* **1981**, *92*, 3708. (b) Jones, W. D.; Chen, P.; Meyer, T. J. *J. Am. Chem. Soc.* **1992**, *114*, 387.

(8) Duesing, R. D.; Tapolsky, G.; Meyer, T. J. *J. Am. Chem. Soc.* **1990**, *112*, 5378.

0020-1669/95/1334-2725$09.00/0

introduction of ligand bridges.[9-12] For example, in [(PTZ-bpy)-$(CO)_3Re^I$(4,4′-bpy)$Re^I(CO)_3$(bpz)]$(PF_6)_2$ (where 4,4′-bpy is 4,4′-bipyridine and bpz is 2,2′-bipyrazine), $Re^I \rightarrow$ bpy, 4,4′-bpy, bpz excitation and electron transfer leads to redox separation across the 11 Å 4,4′-bpy bridge and formation of [$(PTZ^{+}$-bpy)$(CO)_3$-Re^I(4,4′-bpy)$Re^I(CO)_3(bpz^{-})$].[11]

We have continued to pursue photoinduced redox splitting in ligand-bridged complexes and report here the preparation and photophysical properties of [(PTZ-py)$(CO)_3Re^I$(μ-bbpe)Re^I-$(CO)_3(MQ^+)$]$(PF_6)_3$ (bbpe is 1,2-trans-4-(bis-(4′-methyl-2,2′-bipyridyl)ethene.

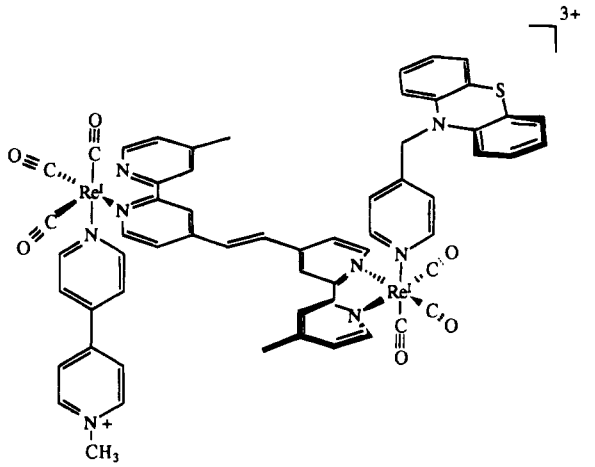

In this complex redox splitting occurs across the bbpe bridging ligand to give [(PTZ-bpy^{+})$(CO)_3$Re(μ-bbpe)Re$(CO)_3(MQ^{\bullet})$]$^{3+}$ following laser flash excitation.

Experimental Section

Materials. The ligands bbpe,[12] py-PTZ,[6] and MQ^+ [6] were prepared as described previously; 4-Etpy (Aldrich) was freshly distilled from KOH prior to use. Tetrahydrofuran (THF) was purified by distillation from Na/benzophenone and stored under argon. Spectral grade acetonitrile (CH_3CN, Burdick and Jackson), 1,2-dichloroethane (DCE, Burdick and Jackson), methanol (Burdick and Jackson), and ethanol (freshly distilled over Mg/I_2) were used for all spectroscopic and electrochemical measurements.

All metal complexes were purified by cation-exchange HPLC chromatography on a Brownlee CX-100 Prep-10 column by utilizing a 4 mM KBr, H_2O-CH_3CN (4:3 v:v)/KH_2PO_4 (pH 7.0) buffered linear gradient controlled by a Perkin-Elmer series-4 pump control unit and monitored at a Perkin Elmer LC-95 variable UV−vis spectrophotometer detector fitted with a 4.5 μL pathlength flow cell. Concentrated 1 mL samples were exchanged onto the column resin in H_2O-CH_3CN (4:3, v:v)/KH_2PO_4 buffer. Ramp gradient and run times varied with the charge on the complex. Typically a 15 min ramp from 0 to 4 mM KBr was employed to effect separation. The major fraction was isolated as the center fraction and metathasized to the PF_6^- salt by the addition of a saturated aqueous solution of NH_4PF_6 prior to photophysical studies.

Possible evidence was found in the HPLC chromatograms for two structural conformers of the possible four diastereoisomers. Separation of the two observed bands could be accomplished by varying the ramp conditions or the implementation of a double ramp. The major component constituted ~90% of the material prior to purification and yielded a single band on the HPLC after purification, indicating that the sample was isomerically pure. After separation by HPLC, the eluted products were precipitated as PF_6^- salts by addition of aqueous $[NH_4](PF_6)$. Analytical HPLC was used to verify sample purity before photophysical measurements were conducted. Chemical analyses were performed by Oneida Research Services.

Measurements. UV−vis spectra were measured in CH_3CN on a Cary Model 14 spectrophotometer interfaced to an IBM PC by On-Line Systems, Inc. IR spectra were recorded on samples prepared as Nujol mulls between NaCl plates on a Mattson Galaxy Series FTIR 5000. Spectrometer control was provided by a Macintosh IIfx. ^1H NMR spectra were recorded on a Varian XL-400 or Brüker AC200 spectrometer. Corrected emission spectra were recorded on a Spex Fluorolog-2 emission spectrometer equipped with a 450-W xenon lamp and a cooled nine-stage Hamamatsu R928 or R446 photomultiplier. Optical response characteristics and PMT response were corrected with a calibration curve generated at 2.0 mm slits by using a NIST calibrated 250-W Ze lamp (Optronics Laboratories, Inc. Model 220M), controlled by a precision current source at 6.50 W (Optronics Laboratories, Inc. Model 65). Room temperature spectra were obtained in 1-cm pathlength quartz cells for CH_3CN or DCE solutions at 298 ± 2 K. Spectra were obtained at 77 ± 2 K in 4:1 (v:v) ethanol−methanol glasses immersed in liquid N_2 in a quartz finger dewar. Low temperature (150−290 K) spectra in 4:1 (v:v) ethanol−methanol were obtained by using a Janis NDT-6 cryostat controlled by a Lakeshore DRC-84C temperature controller. Temperatures were equilibrated for 30−45 min and monitored with an external temperature probe (±3K).

Emission quantum yields (ϕ_{em}) were measured relative to [Ru(bpy)$_3$]-$(PF_6)_2$ in CH_3CN ($\phi'_{em} = 0.062$) and were calculated by eq 1.[13] In eq.

$$\phi_{em} = \phi'_{em}\left(\frac{I}{I'}\right)\left(\frac{A'}{A}\right)\left(\frac{n}{n'}\right)^2 \quad (1)$$

1, I (sample) and I' (standard) are the integrated emission intensities, A and A' are the absorbances at the excitation wavelength, and n and n' are the refractive indices of the solvent.

Time-resolved emission measurements were obtained by using a PRA LN 1000/LN102 nitrogen laser/dye laser combination for sample excitation. The emission was monitored at a right angle to the excitation source by using a PRA B204-3 monochromator with a cooled, 10-stage, Hamamatsu R928 PMT. Transient absorption difference spectra were measured by using a PDL-2 pulsed dye laser (Coumarin 460 dye) pumped by a Quanta-Ray DCR-2A Nd-YAG laser with an excitation pulse of ~6 ns at <5 mJ/pulse. The excitation beam was coincident to an Applied Photophysics laser kinetic spectrometer, which utilized at 250-W pulsed Xe arc lamp as a probe beam, quartz optics, a f/3.4 grating monochromator, and a five-stage, cooled PMT. The outputs for the laser experiments were coupled to either a LeCroy 9400 digital oscilloscope or a LeCroy 6880 digitizer interfaced to an IBM PC. The measurements were made on argon sparged CH_3CN solutions (1×10^{-5} M) in 1-cm pathlength square cuvettes. Transient emission and absorption data were fit by utilizing a global minimization routine based on a modified Levenburg−Marquardt nonlinear, least-squares iterative fitting procedure.[14]

Resonance Raman spectra were obtained on ~10^{-3} M samples in CH_3CN or CH_2Cl_2 at 298 K. The spectra were acquired on spinning samples by using a 135° backscattering geometry. Laser excitation was supplied by a Spectra-Physics 165-05 Ar^+ or a Coherent INNOVA 90 K Kr^+ laser. The scattered radiation was dispersed by a Jobin Yvon U1000 (Instruments SA) double monochromator and detected by a thermoelectrically cooled Hamamatsu R943-02 photomultiplier tube. The resulting signal was processed by a Spectra Link photon counting system (Instruments SA). Data acquisition was controlled by an IBM PS-2 Model 80 computer with Enhanced Prism software (Instruments SA). Raman bands of the solvent served as internal frequency and intensity references.

(9) (a) Furue, M. Yoshidzumi, T.; Kinoshita, S.; Kushada, T.; Nazakura, S.; Kamachi, M. *Bull. Chem. Soc. Jpn.* **1991**, *69*, 1632. (b) Serroni, S.; Denti, G.; Campagna, S.; Juris, A.; Ciano, N.; Balzani, V. *Agnew. Chem., Int. Ed. Engl.* **1992**, *31*, 1495. (c) Scandola, F.; Argazzi, R.; Balzani, C. A.; Chiorboli, C.; Indelli, M. T.; Rampi, M. A. *Coord. Chem. Rev.* **1993**, *125*, 283.

(10) (a) Schanze, K. S.; Sauer, K. *J. Am Chem. Soc.* **1988**, *110*, 1180. (b) Vassilian, A.; Wishart, J. F.; Van Hemelryck, B.; Schwartz, H.; Isied, S. S. *J. Am. Chem. Soc.* **1990**, *112*, 7278.

(11) Tapolsky, G.; Duesing, R.; Meyer, T. J. *J. Phys. Chem.* **1989**, *93*, 3885.

(12) (a) Boyde, S.; Strouse, G. F., Jones, W. E.; Meyer, T. J. *J. Am. Chem. Soc.* **1991**, *112*, 7395. (b) Strouse, G. F.; Schoonover, J. R.; Boyde, S.; Duesing, R.; Jones, W. E.; Meyer, T. J. *Inorg. Chem.*, in press.

(13) Caspar, J. V.; Meyer, T. J. *J. Am. Chem. Soc.* **1989**, *111*, 7448.

(14) Danielson, E. Unpublished results.

Transient resonance Raman spectra were measured by using the third harmonic (354.7 nm) of the Quanta-Ray DCR-2A pulsed Nd:YAG laser as the excitation source as well as the source for the Raman scattering or excitation at 354.7 nm with use of the second harmonic (532 nm) as the source for Raman scattering. The samples (~10–20 mM) were degassed by three cycles of freeze–pump–thawing and sealed in an NMR tube. The scattered radiation was collected in a 135° backscattering geometry into a SPEX 1877 triplemate spectrometer equipped with a 1200 or 1800 grooves/mm grating. The signal was detected by a Princeton Instruments IRY-700G optical multichannel analyzer operating in the gated mode with a ST-110 OSMA detector controlled or a Princeton Instruments intensified CCD operating in the gated integrated mode with a ST-130 controller. Timing was controlled by a Princeton Instruments FG-100 pulse generator. The final spectra are the result of a 5–16 min total integration time. Laser power was between 3 and 5 mJ per pulse. Data collection and storage were controlled by IBM AT or Gateway 2000 computers by using Princeton Instruments software.

Electrochemical measurements were carried out in a N_2 drybox by using a EG&G PAR Model 173 potentiostat and Model 175 waveform generator or a EG&G PAR Model 273 potentiostat. Potentials were measured at a 4 mm diameter Pt disk electrode relative to $Ag/AgNO_3$ (0.1 M). The measured potential under identical conditions for the ferrocenium/ferrocene couple in CH_3CN 0.1 M in $[N(n\text{-}C_4H_9)_4](PF_6)$ was +0.09 V.

Synthesis. Preparation of $[Re(CO)_5(OSO_2CF_3)]$ (I). The Re^I pentacarbonyl triflato species was prepared by a modified version of the procedure of Trogler et al.[15] To a N_2 charged round bottom flask containing CH_2Cl_2 (140 mL) was added $[Re(CO)_5Cl]$ (2.0 g, 5.5 mmol) and the mixture stirred at 298 K for 15 min. An excess of solid $AgOSO_2CF_3$ (1.8 g, 7.0 mmol) was added slowly under a flow of N_2, producing an orange-colored solution which was stirred in the dark for 1.5 h. The product was isolated by removal of AgCl by filtering through Celite and precipitation as a white powder by the slow addition of petroleum ether. Yield: 2.63 g, 99%. IR (CH_2Cl_2): ν_{CO} 2167, 2059, 2031, 2005 cm^{-1}; ν_{SO} 1342, 1178, 1007 cm^{-1}; ν_{CF} 1234, 1202 cm^{-1}.

Preparation of $[Re(CO)_5(py\text{-}PTZ)](OSO_2CF_3)\cdot 3H_2O$ (II). A slightly less than equimolar concentration of **I** (0.62 g, 1.3 mmol) was combined with py-PTZ (0.46 g, 1.58 mmol) in a N_2 charged flask containing 80 mL of CH_2Cl_2 and allowed to stir at room temperature for 48 h. The product was evaporated to dryness and purified by fractional recrystallization from CH_2Cl_2/pentane, producing long yellow needles. Yield: 0.80g, 70%. IR (CH_2Cl_2): ν_{CO} 2164, 2102, 2057, 2022 cm^{-1}. NMR (CD_2Cl_2): 5.82 (s), 6.70 (d,d); 6.7–7.2 (m), 7.59-(d), 8.7 (d). Anal. Calcd for $ReC_{24}H_{20}N_2O_{10}S_2F_3$: C, 35.16; H, 1.70; N, 3.40. Found: C, 35.17; H, 1.71; N, 3.33.

Preparation of $[Re(CO)_5(4,4'bpy)](OSO_2CF_3)\cdot 2H_2O$ (III). Preparation of **III** was carried out as described above except that a 10-fold excess of 4,4′-bipyridine was used to minimize coupled products. The excess 4,4′-bipyridine was removed via successive ether washes. Fractional recrystallization by the addition of pentane dropwise to a concentrated CH_2Cl_2 solution of **III** at 0 °C produced white needles. Yield: 69%. IR (CH_2Cl_2): ν_{CO} 2165, 2102, 2057, 2025 cm^{-1}. NMR (CD_2Cl_2): 7.95 (d), 8.10 (d), 8.8 (d), 9.26 (d). Anal. Calcd for $ReC_{16}H_{12}N_2O_{10}SF_3$: C, 28.79; H, 1.56; N, 4.20. Found: C, 28.76; H, 1.08; N, 3.97.

Preparation of $[Re(CO)_5(4\text{-}Etpy)](OSO_2CF_3)$ (IV). Preparartion of **IV** was carried out as described above. Recrystallization from CH_2Cl_2/pentane produced white crystals. Yield: 72%. IR (CH_2Cl_2): ν_{CO} 2165, 2104, 2057, 2023 cm^{-1}. NMR(acetone-d_6): 1.26 (t), 2.78 (q), 7.58 (d), 9.14 (d). Anal. Calcd for $ReC_{13}H_9NO_8SF_3$: C, 26.81; H, 1.56; N, 2.40. Found: C, 26.88; H, 1.48; N, 2.30.

Preparation of $[Re(CO)_3(py\text{-}PTZ)(bbpe)](PF_6)\cdot 2\,H_2O$ (V). To an argon-sparged solution of THF (5 mL) and bbpe (0.660 g, 1.82 mmol) at reflux was added **II** (0.494 g, 0.802 mmol) in 40 mL of THF dropwise over 2 h. The reaction was heated at reflux for an additional 3 h, cooled to room temperature, and evaporated to dryness. The product was loaded onto an 8 in. alumina gel (neutral) column in a minimum of 3:7 (v:v) CH_3CN–toluene, the first band eluted with 3:7 (v:v) CH_3CN–toluene, the second fraction, containing the desired product, with 2:3 (v:v) CH_3CN–toluene, and a final fraction was removed with MeOH. The second fraction was isolated by concentration of the CH_3CN and precipitation with ether. Cation HPLC was performed to verify the purity of the material. Yield: 0.43 g, 39%. IR (CH_2Cl_2): ν_{CO} 2034, 1934, 1925 cm^{-1}. NMR (CD_3CN): 2.60 (s), 5.08 (s), 6.6 (s), 6.9–7.4 (m), 7.6 (s), 7.9 (s), 8.3–9.3 (m). Anal. Calcd for $ReC_{45}H_{38}N_6O_5SPF_6$: C, 48.87; H, 3.46; N, 7.66. Found: C, 48.20; H, 3.10; N, 7.22.

Preparation of $[(py\text{-}PTZ)(CO)_3Re(\mu\text{-}bbpe)Re(CO)_3(py\text{-}PTZ)](PF_6)_2$ (VI). Preparation of **VI** was conducted as described above, however the bbpe ligand in THF was added dropwise to a refluxing solution of **II**. The final product was purified by cation exchange HPLC chromatography. Yield: 49%. IR(CH_2Cl_2): ν_{CO} 2035, 1935, 1927 cm^{-1}. NMR (CD_3CN): 2.62 (s), 5.08 (s), 6.57(d), 6.8–7.1 (m), 7.29 (d), 7.63 (d), 7.85 (s), 8.12 (d), 8.5 (s), 8.70 (s), 9.05 (d), 9.20 (d). Anal. Calcd for $Re_2C_{66}H_{48}N_8O_6S_2P_2F_{12}$: C, 44.65; H, 2.65; N, 6.30. Found: C, 44.63; H, 2.35; N, 6.31.

Preparation of $[(4\text{-}Etpy)(CO)_3Re(\mu\text{-}bppe)Re(CO)_3(4\text{-}Etpy)](PF_6)_2\cdot H_2O$ (VII). The preparation of **VII** was carried out as for **V**, by reacting **IV** with the bbpe ligand. The final product was purified by cation exchange HPLC chromatography. Yield: 52%. IR (CH_2Cl_2): ν_{CO} 2036, 1933, 1926 cm^{-1}. NMR (CD_2Cl_2): 1.15 (t), 2.62 (q), 2.70 (s), 7.14 (d), 7.57 (d), 7.9–8.1 (m), 8.59 (s), 8.79 (s), 8.81 (s), 8.95 (d), 9.13 (d). Anal. Calcd for $Re_2C_{44}H_{38}N_6O_6P_2F_{12}$: C, 37.0; H, 2.82; N, 5.90. Found: C, 36.71; H, 2.67; N, 6.20.

Preparation of $[py\text{-}PTZ)(CO)_3(Re^I(\mu\text{-}bbpe)Re^I(CO)_3(MQ^+)](PF_6)_3$ (VIII). Preparation of **VIII** was carried out by methylation of the intermediate $[(PTZ\text{-}py)(CO)_3Re(\mu\text{-}bbpe)Re(CO)_3(4,4'\text{-}bpy)](PF_6)_2$ (**IX**). Separation of +1, +2, and 0 charged materials in the complex reaction mixture was achieved by HPLC and a two-step ramp: 0–2 mM and 2–4 mM. Elution of the desired +3 ion was accomplished with 4 mM KBr. Preparation of **IX** was carried out by slow addition of an excess of **III** (0.09 g, 0.143 mmol) in 50 mL of CH_2Cl_2 to an argon-sparged solution of **V** (0.105 g, 0.093 mmol) in refluxing THF (60 mL). The reaction mixture was heated at reflux for 4 h and concentrated by evaporation and the material isolated by precipitation with petroleum ether. HPLC analysis of the products revealed two major components. No attempt to isolate the components was attempted.

Conversion of **IX** to **VIII** was carried out by addition of excess MeI (10 mL, distilled) in 20 mL of dry DMF, stirring at room temperature for 24 h (resulting in a color change from yellow to orange), and heating at reflux for 4 h. The DMF and CH_3I were removed under vacuum. The resulting orange solid was metathasized to the PF_6^- salt by dissolving in H_2O/MeOH, filtering and treating with a saturated aqueous solution of NH_4PF_6. The orange solid was dissolved in dry acetone and converted to the Cl^- salt by addition of $[N(n\text{-}C_4H_9)_4]Cl$. The Cl^- salt was purified by HPLC chromatography on a weak cation exchange, semiprep column (Brownlee CX-100 Prep-10). The major component of the +3 ion was collected by eluting with an 8 mM KBr, CH_3CN/KH_2PO_4 buffered linear gradient (pH 7.0), with the eluent monitored at 430 and 355 nm. Metathesis of the Br^- salt to the PF_6^- salt was carried out by the addition of an aqueous solution of NH_4PF_6. Yield: 0.013g, 8% based on **V**. IR (CH_2Cl_2): ν_{CO} 2033, 1934, 1924 cm^{-1}. NMR (CD_2Cl_2): 2.65 (s), 4.81 (s), 5.1 (s), 6.4–6.6 (m), 6.8–7.4 (m), 7.65 (d), 7.8 (s), 7.85 (m), 8.15 (d,d), 8.27 (s), 8.88 (s), 9.0 (d), 9.2 (d). Anal. Calcd for $Re_2C_{59}H_{45}N_8O_6SP_3F_{18}$: C, 39.34; H, 2.52; N, 6.22. Found: C, 40.10; H, 2.65; N, 5.95.

Results

Absorption spectra in CH_3CN at 298 ± 2 K are presented in Figure 1. The bands at ~380 nm arise from overlapping $d\pi \rightarrow \pi^*$(bbpe) MLCT transitions and the bands at <320 nm from overlapping $d\pi \rightarrow \pi^*$(pyridyl) and $\pi \rightarrow \pi^*$(bbpe) transitions. Absorption maxima and extinction coefficients in CH_3CN at 298 ± 2 K are listed in Table 1, as are $E_{1/2}$ values in 0.1M $[N(n\text{-}C_4H_9)_4](PF_6)$–$CH_3CN$ at a scan rate of 100 mV/s. The first bbpe-based reductions in the Re^I complexes were reversible, except in $[(py\text{-}PTZ)(CO)_3Re(\mu\text{-}bbpe)Re(CO)_3(MQ^+)]^{3+}$ where reduction resulted in precipitation at the electrode, characterized

(15) (a) Trogler, W. C. *J. Am. Chem. Soc.* **1979**, *101*, 6459. (b) Trogler, W. C. *Inorg. Synth.* **1989**, *26*, 113.

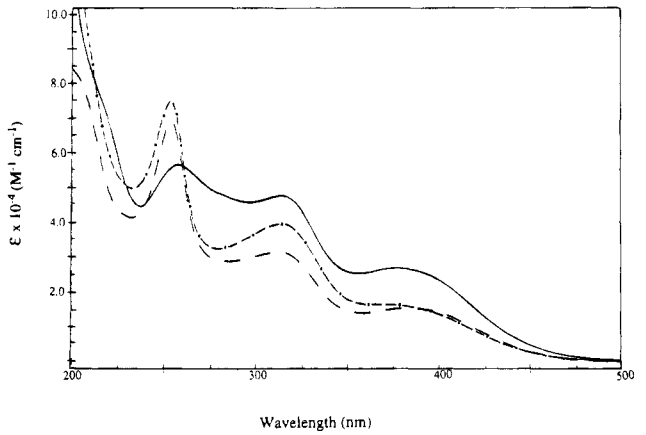

Figure 1. Absorption spectra in CH_3CN at 298 ± 2 K for (A, —) $[(4\text{-Etpy})(CO)_3Re(\mu\text{-bbpe})Re(CO)_3(4\text{-Etpy})](PF_6)_2$, (B, — · —) $[(py\text{-}PTZ(CO)_3Re^{I}(\mu\text{-bbpe})Re^{I}(CO)_3(py\text{-}PTZ)](PF_6)_2$, and (C, — —) $[(py\text{-}PTZ)(CO)_3Re^{I}(\mu\text{-bbpe})Re^{I}(CO)_3(MQ^+)](PF_6)_3$.

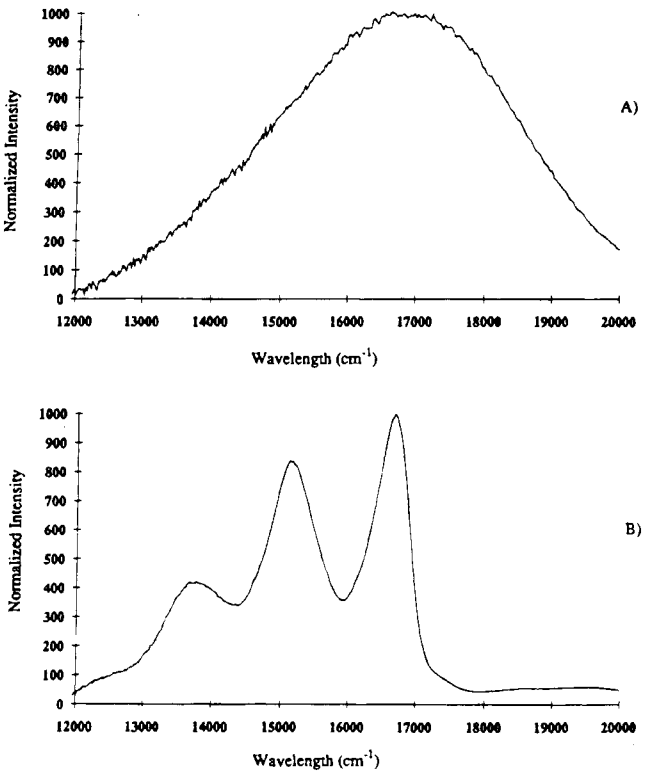

Figure 2. Emission spectra in 4:1 (v:v) ethanol—methanol of $[(4\text{-Etpy})(CO)_3Re(\mu\text{-bbpe})Re(CO)_3(4\text{-Etpy})](PF_6)_2$ at (A) 298 K and (B) 77 K.

by a current spike on the reverse scan. For complexes containing PTZ, the appearance of the second irreversible PTZ-based oxidation wave obscured the $Re^{II/I}$ oxidation waves in the bbpe complexes as observed earlier in related complexes.[6]

Emission Spectra and Excited State Properties. In Figure 2 are shown emission spectra for $[(4\text{-Etpy})(CO)_3Re(\mu\text{-bbpe})Re(CO)_3(4\text{-Etpy})](PF_6)_2$ (1×10^{-6} M) at 298 ± 2 K and 77 ± 2 K in 4:1 (v:v) ethanol—methanol. The emission bandshape and quantum yields for $[(4\text{-Etpy})(CO)_3Re(\mu\text{-bbpe})Re(CO)_3(4\text{-Etpy})](PF_6)_2$ did not vary with excitation energy from λ_{ex} = 355 to 420 nm. Emission maxima and quantum yields are presented in Table 2 along with data for model complexes. A structured emission was observed for $[(py\text{-}PTZ)(CO)_3Re(\mu\text{-bbpe})Re(CO)_3(py\text{-}PTZ)]^{2+}$ at 77 ± 2 K in 4:1 (v:v) ethanol—methanol, which was similar to the emission from $[(4\text{-Etpy})(CO)_3Re(\mu\text{-bbpe})Re(CO)_3(4\text{-Etpy})]^{2+}$ under the same conditions. No observable emission was detected from solutions containing

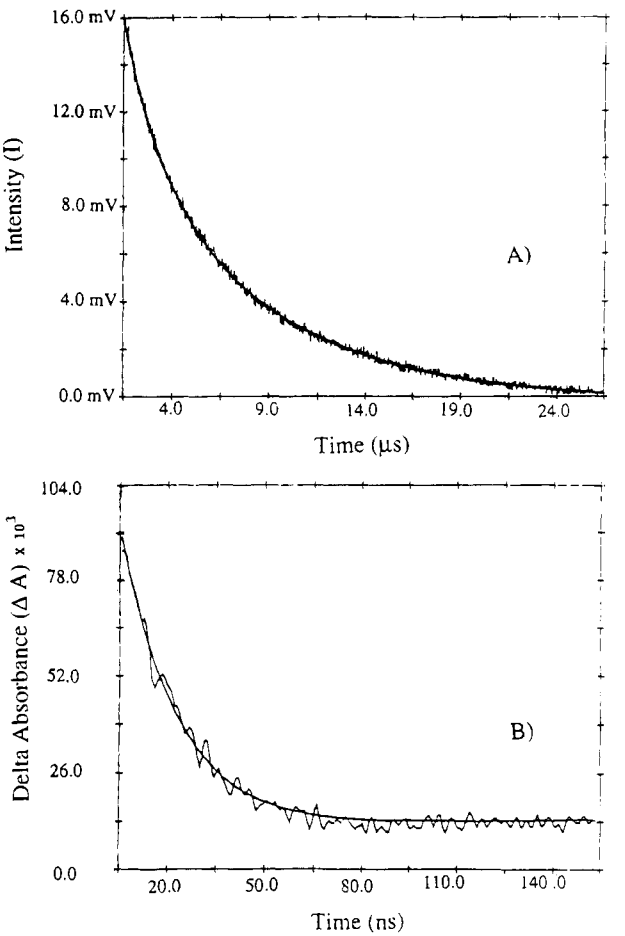

Figure 3. (A) Time-resolved emission decay from $[(4\text{-Etpy})(CO)_3Re(\mu\text{-bbpe})Re(CO)_3(4\text{-Etpy})](PF_6)_2$ at 109 ± 2 K in 4:1 (v:v) ethanol—methanol. Fits of the data to eq 2 are shown as the solid line with the parameters $I_a = 9.3 \times 10^{-3}$, $k_a = 9.37 \times 10^4\ s^{-1}$, $I_b = 5.6 \times 10^{-3}$, $k_b = 3.5 \times 10^5\ s^{-1}$. (B) Single exponential, time-resolved absorption changes at 510 nm following 420 nm laser flash excitation (<4 μJ/pulse) of $[(py\text{-}PTZ)(CO)_3Re(\mu\text{-bbpe})(CO)_3(py\text{-}PTZ)](PF_6)_2$ at 298 ± 2 K in CH_3CN. The kinetic fit was to eq 4 with $A(t) = (7.9 \times 10^{-2})\exp(-2.4 \times 10^7 t)$.

$[(py\text{-}PTZ)(CO)_3Re(\mu\text{-bbpe})Re(CO)_3(py\text{-}PTZ)]^{2+}$ or $[(py\text{-}PTZ)(CO)_3Re(\mu\text{-bbpe})Re(CO)_3(MQ^+)]^{3+}$ at 298 ± 2 K in CH_3CN.

Emission decay lifetimes are also reported in Table 2. For $[Re(bbpe)(CO)_3(4\text{-Etpy})](PF_6)$ and $[(4\text{-Etpy})(CO)_3Re(\mu\text{-bbpe})Re(CO)_3(4\text{-Etpy})](PF_6)_2$, excited state decays were non-exponential but could be fit satisfactorily to the biexponential function in eq 2. A fit is illustrated in Figure 3A. In Supplemental Table 1 are listed both rate constants and preexponential terms expressed as fractions of the total intensity change obtained from these fits for $[(4\text{-Etpy})(CO)_3Re(\mu\text{-bbpe})Re(CO)_3(4\text{-Etpy})](PF_6)_2$ in 4:1 (v:v) ethanol—methanol as a function of temperature. In Figure 4 is shown a plot illustrating how the two fractions, eq 3, vary with temperature between 160—298 K.

$$I(t) = I_a \exp(-k_a t) + I_b \exp(-k_b t) \quad (2)$$

$$F_A = \frac{I_a}{I_a + I_b}$$

$$F_B + F_A = 1 \quad (3)$$

In Figure 5 are shown transient absorption difference spectra for $[(4\text{-Etpy})(CO)_3Re(\mu\text{-bbpe})Re(CO)_3(4\text{-Etpy})](PF_6)_2$, [(py-

Table 1. Electrochemical and Spectral Data in CH_3CN at 298 ± 2 K

salt	$E_{1/2}$, V[a] $Re^{II/I}$	$PTZ^{+/0}$	$MQ^{0/-}$	$bpy^{0/-}$	λ_{max}, nm ($\epsilon \times 10^{-4}$ M^{-1} cm^{-1})[b]	transition
$[Re(bpy)(CO)_3(4\text{-Etpy})](PF_6)$[c]	+1.72			−1.17	308 (1.2)	$\pi \rightarrow \pi^*$ (4-Etpy, bpy)
					320 (1.3)	$\pi \rightarrow \pi^*$ (4-Etpy, bpy)
					350 (4.0)	$d\pi \rightarrow \pi^*$ (bpy)
$[Re(bpy)(CO)_3(py\text{-}PTZ)](PF_6)$[c]	+1.60	+0.83		−1.13	308 (1.7)	$\pi \rightarrow \pi^*$ (PTZ-py, bpy)
					320 (1.7)	$\pi \rightarrow \pi^*$ (PTZ-py, bpy)
					350 (4.5)	$d\pi \rightarrow \pi^*$ (bpy)
$[Re(bpy\text{-}PTZ)(CO)_3(MQ^+)](PF_6)_2$[d]	e	+0.84	−0.70	−1.20		
$[(4\text{-Etpy})(CO)_3Re(\mu\text{-bbpe})Re(CO)_3(4\text{-Etpy})](PF_6)_2$	+1.70			−1.05	318 (4.3)	$\pi \rightarrow \pi^*$ (4-Etpy, bbpe)
					376 (2.4)	$\pi \rightarrow \pi^*$, $d\pi \rightarrow \pi^*$ (bbpe)
$[(py\text{-}PTZ)(CO)_3Re(\mu\text{-bbpe})Re(CO)_3(py\text{-}PTZ)](PF_6)_2$	e	+0.76		−1.05	314 (3.1)	$\pi \rightarrow \pi^*$ (py-PTZ, bbpe)
					384 (1.4)	$\pi \rightarrow \pi^*$, $d\pi \rightarrow \pi^*$ (bbpe)
$[(py\text{-}PTZ)(CO)_3Re(\mu\text{-bbpe})Re(CO)_3(MQ^+)](PF_6)_3$	e	+0.80	−0.69	−1.10[f]	315 (4.0)	$\pi \rightarrow \pi^*$ (MQ^+, bbpe)
					388 (1.7)	$\pi \rightarrow \pi^*$ (bbpe)
						$d\pi \rightarrow \pi^*$ (MQ^+, bbpe)

[a] From cyclic voltammetric measurements on 0.1 M $[N(n\text{-}C_4H_9)_4(PF_6)]-CH_3CN$ solutions vs SSCE at a 4 mm Pt disk electrode at 100 mV/s; $E_{1/2}$ for $[Fe(C_5H_5)_2]^{+/0} = 0.307$ V measured under the same conditions. [b] From measurements on solutions in the range 1×10^{-6} to 6×10^{-6} M. [c] Chen, P.; Westmoreland, T. D.; Danielson, E.; Schanze, K. S.; Anthon, D.; Neveux, P. E.; Meyer, T. J. *Inorg. Chem.* **1987**, *26*, 1116. [d] Duesing, R. Ph.D. Dissertation, The University of North Carolina at Chapel Hill, 1988. [e] The $Re^{II/I}$ couple was obscured by the second oxidation of -PTZ which is irreversible. [f] $E_{p,c}$ is reported for the reduction at bbpe in $[[(py\text{-}PTZ)(CO)_3Re(\mu\text{-bbpe})Re(CO)_3(MQ^+)]^{3+}$ rather than $E_{1/2}$, due to precipitation of the reduced material onto the electrode. A spike occurs for the return, oxidative component of the wave.

Table 2. Excited State Properties

salt	medium[a]	λ_{em}, nm (ϕ_{em}) (±2 nm)	τ (ns)[b] (±3%)	k_{bet} ($\times 10^7$ s^{-1})[c] (±3%)
$[Re(bpy)(CO)_3(4\text{-Etpy})](PF_6)$[d]	CH_3CN, 298 K	590 (0.027)	220	
	DCE, 298 K	570 (0.014)	505	
	4:1 (v:v) E−M, 298 K	588 (0.017)	176	
	4:1 (v:v) E−M, 77 K	515	4550	
$[Re(bpy)(CO)_3(py\text{-}PTZ)](PF_6)$[d]	CH_3CN, 298 K			3.33
	DCE, 298 K			1.11
$[Re(bpy\text{-}PTZ)(CO)_3(MQ^+)](PF_6)_2$[e]	CH_3CN, 298 K			>10
	DCE, 298 K			>10
$[(4\text{-Etpy})(CO)_3Re(\mu\text{-bbpe})Re(CO)_3(4\text{-Etpy})](PF_6)_2$	CH_3CN, 298 K	595 (0.004)	172 ($I_a = 0.145$)[f]	
			12 ($I_b = 0.750$)	
	DCE, 298 K	605 (0.005)	572 ($I_a = 0.012$)[f]	
			34 ($I_b = 0.025$)	
	4:1 (v:v) E−M, 298 K	585 (0.001)	180 ($I_a = 0.140$)[f]	
			18 ($I_b = 2.61$)	
	4:1 (v:v) E−M, 77 K	600	14200 ($I_a = 0.011$)[f]	
			1950 ($I_b = 0.012$)	
$[(py\text{-}PTZ)(CO)_3Re(\mu\text{-bbpe})Re(CO)_3(py\text{-}PTZ)](PF_6)_2$	CH_3CN, 298 K		[g]	2.33
	DCE, 298 K			1.82
	4:1 (v:v) E−M, 298 K		[g]	
	4:1 (v:v) E−M, 77 K	600	20130 ($I_a = 0.140$)[f]	
			5290 ($I_b = 0.126$)	
$[(py\text{-}PTZ)(CO)_3Re(\mu\text{-bbpe})Re(CO)_3(MQ^+)](PF_6)_3$	CH_3CN, 298 K		[g]	5.56
	DCE, 298 K			3.03

[a] DCE is 1,2-dichloroethane, and E−M is 4:1 (v:v) ethanol−methanol. [b] Emission decay lifetimes were fit satisfactorily to the single exponential decay function, $I(t) = I_0 \exp(-t/\tau)$, where τ was the lifetime and I_0 the emission intensity at $t = 0$. [c] k_{bet} is the rate constant for back electron transfer from the redox separated state to the ground state by time resolved transient absorption measurements, see text. The decays could be satisfactorily fit to eq 4. [d] Reference 6a. Chen, P. Ph.D. Dissertation, The University of North Carolina at Chapel Hill, 1989. [e] Duesing, R. Ph.D. Dissertation. The University of North Carolina at Chapel Hill, 1988. [f] The decays were complex but could be fit satisfactorily to the biexponential expression, $I(t) = I_a \exp(-k_a t) + I_b \exp(-k_b t)$. The rate constants from the fits are cited as is the fraction of emitted intensity associated with each as calculated by eq 3. [g] There is no emission by steady state or flash photolysis.

$PTZ)(CO)_3Re(\mu\text{-bbpe})Re(CO)_3(py\text{-}PTZ)](PF_6)_2$, and $[(py\text{-}PTZ)(CO)_3Re(\mu\text{-bbpe})Re(CO)_3(MQ^+](PF_6)_3$ in DCE obtained 20 ns following 420 nm excitation (4 mJ/pulse). The transient difference spectrum for $[Cl(CO)_3Re(\mu\text{-bbpe})Re(CO)_3Cl]$ was also acquired and found to be similar to that observed for $[(4\text{-Etpy})(CO)_3Re(\mu\text{-bbpe})Re(CO)_3(4\text{-Etpy})](PF_6)_2$ in Figure 5, but with maxima appearing at 365 and 480 nm. The decays of the transient absorption changes were time-resolved following excitation at 420 nm. The decays could be fit satisfactorily to the single exponential function in eq 4, where A_0 was the

$$A_t = A_0 \exp(-kt) \quad (4)$$

absorbance at $t = 0$. The decay of $[(py\text{-}PTZ)(CO)_3Re(\mu\text{-bbpe})Re(CO)_3(py\text{-}PTZ](PF_6)_2$ is shown in Figure 3B.

Resonance Raman and Transient Resonance Raman. Raman band energies from ground state (cw, 363.8 nm excitation) and transient resonance Raman spectra (354.7 nm pulse and probe) are listed in Table 3. Spectra are shown in Figure 6. The ligand origins of the bands were established by comparisons with $MQ^{\bullet}$, $[Re^{I}(bpy)(CO)_3(MQ^{\bullet})]^+$, $[Re^{II}(bpy)(CO)_3(MQ^{\bullet})]^{2+}$ *, $[Re^{I}(CO)_3(bpy)(py\text{-}PTZ^{\bullet+})]^+$, 10-$MePTZ^{\bullet+}$ and $bbpe^{\bullet-}$ (Table 3).[16,17]

In the excitation region 355 − 365 nm for $[(4\text{-Etpy})(CO)_3Re(\mu\text{-bbpe})Re(CO)_3(4\text{-Etpy})](PF_6)_2$, the absorption spectrum is a convolution of $d\pi \rightarrow \pi^*$(bbpe) and $\pi \rightarrow \pi^*$(bbpe) bands. In the cw spectra the most enhanced bands appear at 1028, 1192, 1218, 1285, 1329, 1426, 1491, 1540, 1616, and 1639 cm^{-1} consistent with their assignment as bbpe ground state modes as

(16) Schoonover, J. R.; Chen, P. Y.; Bates, W. D.; Meyer, T. J. Unpublished results.

(17) Schoonover, J. R.; Strouse, G. F.; Chen, P. Y.; Bates, W. D.; Meyer, T. J. *Inorg. Chem.* **1993**, *32* 2618.

Table 3. CW and Transient (355 nm Pulse and Probe) Raman Band Energies for $[(4\text{-Etpy})(CO)_3Re^{I}(\mu\text{-bbpe})Re^{I}(CO)_3(4\text{-Etpy})]^{2+}$ in CH_3CN at 298 K Compared to Electrochemically Prepared $bbpe^{\bullet-}$ and the Transient Spectrum for $[(dmb)_2Ru^{II}(\mu\text{-bbpe})Ru^{II}(dmb)_2]^{4+}$ [a]

$[(4\text{-Etpy})(CO)_3Re^{I}(\mu\text{-bbpe})Re^{I}(CO)_3(4\text{-Etpy})]^{2+}$		$bbpe^{\bullet-}$	$[(dmb)_2Ru^{II}(\mu\text{-bbpe})Ru^{II}(dmb)_2]^{4+}$
pulsed 355 nm	cw 364 nm	cw 568 nm	pulsed 355 nm
1029	1028	1026	1033
		1038	1041
		1129	1128
	1192		1205
1215	1218		1213
		1244	
		1257	1259
	1285		1286
1329	1329	1309	1324
		1363	1345
1384	1426	1433	1425
1445		1446	1443
			1456
1470		1480	1481
1496	1491	1497	1493
1510			
1535	1540		
1556	1555		
1597		1594	1585
1624	1616		1618
1642	1639		

[a] Strouse, G. F.; Boyde, S.; Schoonover, J. R.; Jones, W. E.; Meyer, T. J. *Inorg. Chem.*, in press.

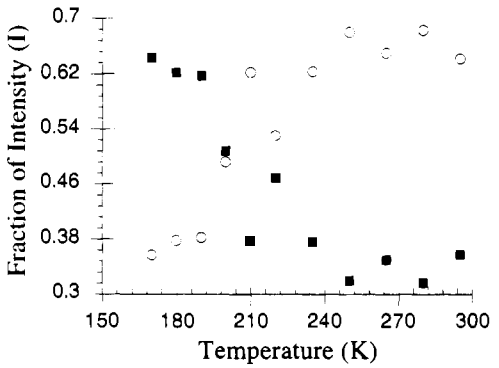

Figure 4. Variations in $F_a = I_a/(I_a + I_b)$ (○) and $F_b = 1 - F_a$ (■), eq 3, from the biexponential fits of the emission decay data for $[(4\text{-Etpy})(CO)_3Re(\mu\text{-bbpe})Re(CO)_3(4\text{-Etpy})](PF_6)_2$ in 4:1 (v:v) ethanol–methanol.

observed in $[(dmb)_2Ru(\mu\text{-bbpe})Ru(dmb)_2](PF_6)_4$ (dmb is 4,4′-dimethyl-2,2′-bipyrine).[12] The band at 1639 cm^{-1} has been assigned to the symmetrical olefin bridge stretch (−C=C−), and the band at 1192 cm^{-1} to the symmetrical ring carbon to double bond stretch (ring-C=).[12,17] In the excited state resonance Raman spectrum of $[(4\text{-Etpy})(CO)_3Re(\mu\text{-bbpe})Re(CO)_3(4\text{-Etpy})](PF_6)_2$ (355 nm/355 nm), new bands attributable to bbpe appear at 1445, 1470, 1496, 1510, 1597, and 1624 cm^{-1} (Table 3).

In the transient spectra of $[(py\text{-}PTZ)(CO)_3Re(\mu\text{-bbpe})Re(CO)_3(py\text{-}PTZ)](PF_6)_2$ and $[(py\text{-}PTZ)(CO)_3Re^{I}(\mu\text{-bbpe})Re^{I}(CO)_3(MQ^+)](PF_6)_3$ bands characteristic of $\text{-PTZ}^{\bullet+}$ appear in the 355 nm/532 nm spectra (Figure 6) at 1022, 1050, 1220, 1250, 1266, 1290, 1566, and 1590 cm^{-1}. For $[(py\text{-}PTZ)(CO)_3Re(\mu\text{-bbpe})Re(CO)_3(py\text{-}PTZ)](PF_6)_2$ characteristic $bbpe^{\bullet-}$ bands (Table 3) are observed in the 355 nm/355 nm spectrum.[12,17] Bands for $MQ^{\bullet}$ appear in the 355 nm/355 nm spectrum of $[(py\text{-}PTZ)(CO)_3Re(\mu\text{-bbpe})Re(CO)_3(MQ^+)](PF_6)_3$ at 807, 992, 1032, 1243, 1359, 1530, and 1650 cm^{-1}.[17] Ground state bbpe bands appear in the excited state spectrum of $[(py\text{-}PTZ)(CO)_3Re(\mu\text{-bbpe})Re(CO)_3(MQ^+)](PF_6)_3$ at 1284, 1493, 1618, and 1642 cm^{-1}.

Discussion

The transient absorption and resonance Raman data provide direct evidence for intramolecular electron transfer and formation of redox-separated states following $d\pi \rightarrow \pi^*(bbpe)$, $d\pi \rightarrow \pi^*(MQ^+)$, $\pi \rightarrow \pi^*(bbpe)$ excitation of $[(py\text{-}PTZ)(CO)_3Re(\mu\text{-bbpe})Re(CO)_3(MQ^+)](PF_6)_3$ and $d\pi \rightarrow \pi^*(bbpe)$, $\pi \rightarrow \pi^*(bbpe)$ excitation of $[(py\text{-}PTZ)(CO)_3Re(\mu\text{-bbpe})Re(CO)_3(py\text{-}PTZ)](PF_6)_2$. The case of greater interest is the donor–acceptor complex, where net photoinduced electron transfer occurs across bbpe as a ligand bridge, eq 5. The final redox-separated state is formed

$$\xrightarrow{h\nu} \left\{ \begin{array}{l} [(py\text{-}PTZ)(CO)_3Re^{I}(\mu\text{-}bbpe^{\bullet})Re^{I}(CO)_3(MQ^+)]^{3+*} \\ [(py\text{-}PTZ)(CO)_3Re^{I}(\mu\text{-}bbpe)Re^{II}(CO)_3(MQ^+)]^{3+*} \\ [(py\text{-}PTZ)(CO)_3Re^{II}(\mu\text{-}bbpe)Re^{I}(CO)_3(MQ^+)]^{3+*} \\ [(py\text{-}PTZ)(CO)_3Re^{I}(\mu\text{-}bbpe)Re^{II}(CO)_3(MQ^{\bullet})]^{3+*} \end{array} \right\} \rightarrow\rightarrow \quad (5)$$

$$[(py\text{-}PTZ^{\bullet+})(CO)_3Re^{I}(\mu\text{-}bbpe)Re^{I}(CO)_3(MQ^{\bullet})]^{3+}$$

within the laser pulse of the apparatus used (<6 ns) following excitation from 355 to 420 nm. Its appearance in the transient absorption difference spectrum in Figure 5 can be inferred from the positive absorption features at ~520 nm for $\text{-PTZ}^{\bullet+}$ and at ~600 nm for $-MQ^{\bullet}$. A closely related spectrum has been reported following $Re^{I} \rightarrow bpy$, MQ^+ excitation of $[Re(CO)_3(bpy\text{-}PTZ)(MQ^+)](PF_6)_2$.[18] The additional feature of lower absorptivity at ~700 nm is a second $\text{-PTZ}^{\bullet+}$ band.

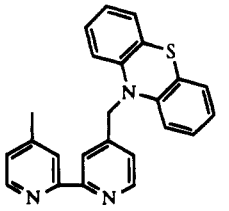

bpy-PTZ

The transient absorption features are broad and the overlap of bands leads to equivocation as to the assignment of the underlying transitions. The transient resonance Raman spectrum obtained 20 ns after 354.7 nm excitation, Figure 6, is consistent with reaction 5. In this spectrum there are bands characteristic

(18) Duesing, R. Ph.D. Dissertation, The University of North Carolina at Chapel Hill, 1990.
(19) Bates, W. D.; Chen, P. Y.; Meyer, T. J. Unpublished results.

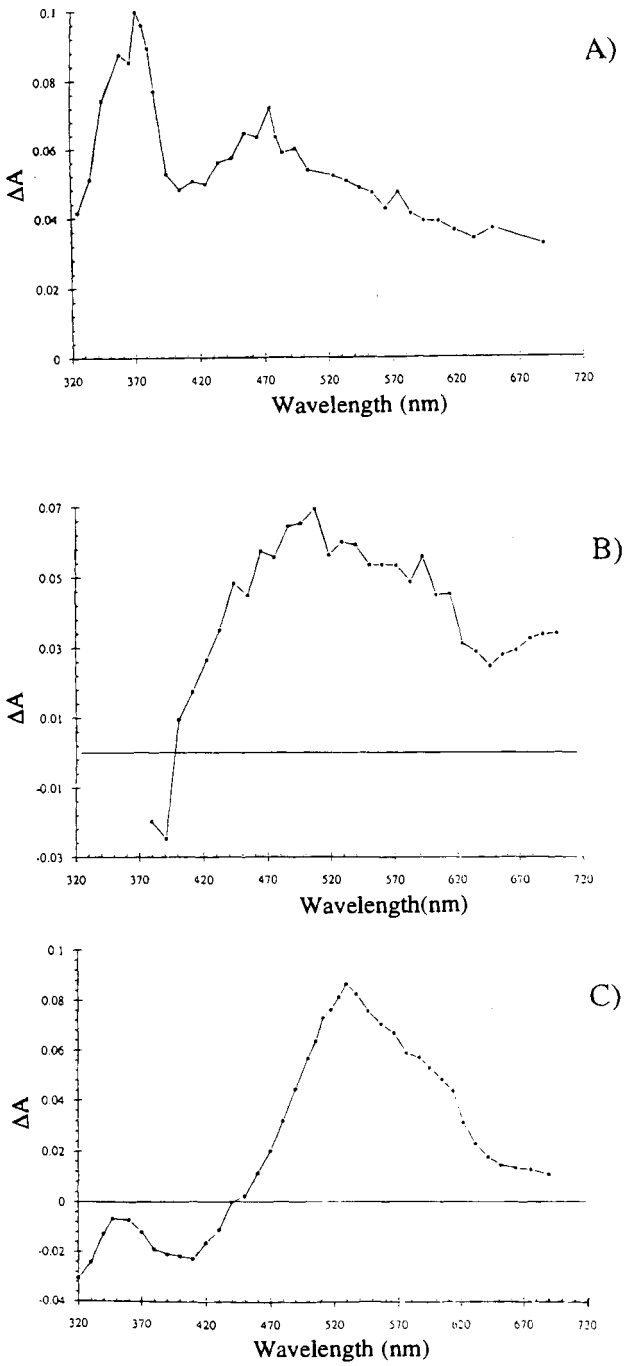

Figure 5. Transient absorbance difference spectra acquired 20 ns after ~4 μJ/pulse excitation at 420 nm in 1,2-DCE for (A) $[(4\text{-Etpy})(CO)_3Re(\mu\text{-bbpe})Re(CO)_3(4\text{-Etpy})](PF_6)_2$, (B) $[(py\text{-}PTZ)(CO)_3Re(\mu\text{-bbpe})Re(CO)_3(py\text{-}PTZ)](PF_6)_2$, and (C) $[(py\text{-}PTZ)(CO)_3Re(\mu\text{-bbpe})Re(CO)_3(MQ^+)](PF_6)_3$.

of -$PTZ^{\bullet+}$, $MQ^{\bullet}$, and ground state bbpe. The latter provide a marker for the Re^I(bbpe) chromophore in the excited state.

The transient spectroscopies reveal that following $Re^I \rightarrow$ bbpe, $Re^I \rightarrow MQ^+$, $\pi \rightarrow \pi^*$(bbpe) excitation, redox separation is achieved by net, long-range, -PTZ→ $-MQ^+$ electron transfer, 13.5 ± 0.5 Å across the bbpe ligand bridge. The electron transfer steps were too rapid to time-resolve with our apparatus. As illustrated for initial $Re^I \rightarrow$ bbpe excitation in Scheme 1, they could involve either initial $bbpe^{\bullet-} \rightarrow -MQ^+$ or -PTZ → Re^{II} electron transfer. Related schemes can be written for sequential electron transfer following $\pi \rightarrow \pi^*$ or $Re^I \rightarrow MQ^+$ excitations. The second electron transfer step in the right hand channel in Scheme 1 must occur by through-space or through bond -PTZ → Re^{II} transfer. A sequential mechanism involving

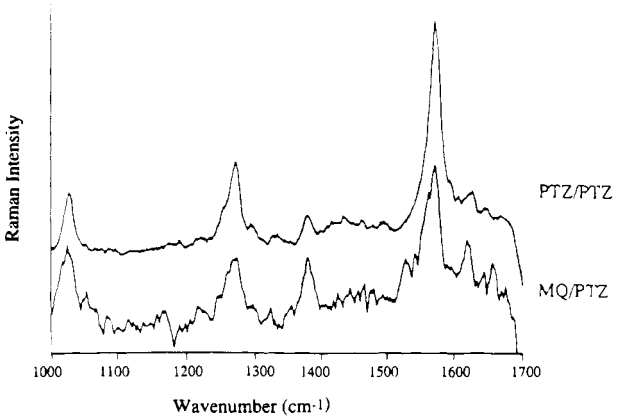

Figure 6. Transient resonance Raman spectra following 355 nm excitation of $[(py\text{-}PTZ)(CO)_3Re(\mu\text{-bbpe})Re(CO)_3(py\text{-}PTZ)](PF_6)_2$ and $[(PTZ\text{-}py)Re(CO)_3(\mu\text{-bbpe})Re(CO)_3(MQ^+)](PF_6)_3$ probed at 532 nm (3–5 mJ/pulse) in CH_3CN.

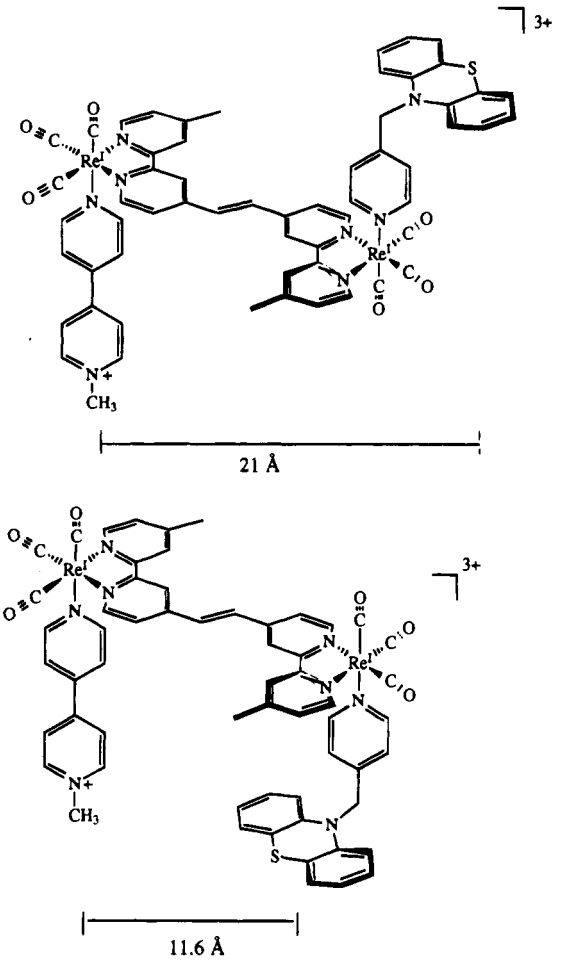

Figure 7. Anti and syn conformers of $[(py\text{-}PTZ)(CO)_3Re(\mu\text{-bbpe})Re(CO)_3(MQ^+)]^{3+}$.

$Re^I \rightarrow Re^{II}$ cross-bridge electron transfer following $Re^I \rightarrow$ bbpe excitation is disfavoured by >0.38 eV in the $Re^I \rightarrow Re^{II}$ step.

Once the $-MQ^{\bullet}$/$-PTZ^{\bullet+}$ redox-separated state is formed, back electron transfer returning to the ground state is relatively rapid with k(DCE, 295 ± 2 K) = (5.6 ± 0.1) × 10^7 s^{-1}. By comparison, back electron transfer in $[(PTZ^{\bullet+}\text{-bpy})Re^I(CO)_3(MQ^{\bullet})]^{3+}$, which forms following MLCT excitation of $[(PTZ\text{-bpy})Re^I(CO)_3(MQ^+)](PF_6)_3$ occurs with $k > 10^8$ s^{-1} in DCE. In this case, the center-to-center distance of closest approach between the center of the heterocyclic rings of MQ^+ and the central ring of -PTZ is ~4–5 Å. There is no experimental

Scheme 1

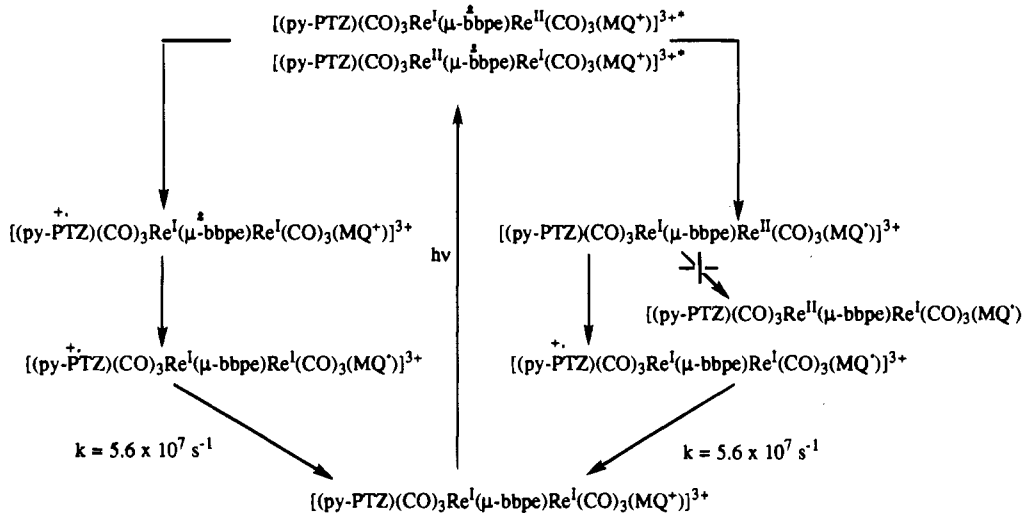

evidence as to whether electron transfer is dominated by through space or through bond electron transfer. In either case, there is a rate decrease of greater than a factor of 3 for the bbpe-bridge case.[18,20,21b] Direct electronic coupling in the π-system by π/π^* mixing is broken by the $-CH_2-$ group in py-PTZ.

Anti and syn conformers are illustrated in Figure 7. They are two of four diastereoisomers in which the chiral Re centers are bridged by bbpe in an elongated form. In one, the shortest center-to-center distance between -PTZ and -MQ^+ is $\sim 11.6 \pm 0.5$ Å. In the other, it is $\sim 21 \pm 1.0$ Å. The other pair of diastereoisomers are the mirror images of the anti and syn conformers arising by rotation around the single bond between the olefin and the bpy subunits. There was HPLC evidence for two forms, but the major fraction (>90%), which was used in the photophysical experiments, gave a single band on repetitive HPLC analysis. Given the relatively rapid rate constant for back electron transfer we assume that the conformers must be freely interconverting with electron transfers dominated by the syn conformer illustrated in Figure 7B.

Intramolecular electron transfer also occurs in [(py-PTZ)-$(CO)_3$Re(μ-bbpe)Re$(CO)_3$(py-PTZ)]$^{2+}$ following d$\pi \rightarrow \pi^*$-(bbpe), $\pi \rightarrow \pi^*$(bbpe) excitation. In this case, a broad absorption centered at ~500 nm appears in the transient absorption difference spectrum with evidence for a shoulder at lower energy. This spectrum is consistent with overlapping bands for -$PTZ^{\bullet+}$ (λ_{max} = 510 nm and 700 nm) and $bbpe^{\bullet-}$ (λ_{max} = 520 nm and >650 nm, as observed in [$(dmb)_2$-$Ru^{III}(bbpe^{\bullet-})Ru^{II}(dmb)_2]^{2+*}$).[12]

In this case, the transient resonance Raman spectrum is also revealing, Figure 6. With 355 nm excitation and a 532 nm probe, bands characteristic of -$PTZ^{\bullet+}$ appear at 1022, 1050, 1217, 1264, 1291, 1566, and 1590 cm^{-1}. The Raman observations are consistent with -PTZ $\rightarrow$ Re^{II} intramolecular electron transfer following d$\pi \rightarrow \pi^*$(bbpe), $\pi \rightarrow \pi^*$(bbpe) excitation as in eq 6. The rate constant for back electron transfer in this case,

$$[(py\text{-}PTZ)(CO)_3Re^{I}(\mu\text{-}bbpe)Re^{I}(CO)_3(py\text{-}PTZ)]^{2+} \xrightarrow{h\nu} \begin{cases} [(py\text{-}PTZ)(CO)_3Re^{I}(\mu\text{-}bbpe^{\bullet-})Re^{I}(CO)_3(py\text{-}PTZ)]^{2+} \\ [(py\text{-}PTZ)(CO)_3Re^{II}(\mu\text{-}bbpe^{\bullet-})Re^{I}(CO)_3(py\text{-}PTZ)]^{2+} \end{cases} \quad (6a)$$

$$\begin{cases} [(py\text{-}PTZ)(CO)_3Re^{I}(\mu\text{-}bbpe^{\bullet-})Re^{I}(CO)_3(py\text{-}PTZ)]^{2+} \\ [(py\text{-}PTZ)(CO)_3Re^{II}(\mu\text{-}bbpe^{\bullet-})Re^{I}(CO)_3(py\text{-}PTZ)]^{2+} \end{cases} \xrightarrow{k > 1 \times 10^8\ s^{-1}} [(py\text{-}PTZ^{\bullet+})(CO)_3Re^{I}(\mu\text{-}bbpe^{\bullet-})Re^{I}(CO)_3(py\text{-}PTZ)]^{2+} \quad (6b)$$

$k = 1.8 \times 10^8\ s^{-1}$ (DCE, 298 K), is nearly the same as in the redox-separated state [(4,4′-$(CONEt_2)_2$bpy$^{\bullet-}$)$Re^{I}(CO)_3$(py-$PTZ^{\bullet+}$)]$^+$ for which the driving force is the same, $\Delta G^0 \sim -1.80$ eV, and the distance of closest approach between the center of the acceptor bipyridine and the center ring of PTZ is ~4.5 Å.[21] The separation distance between -PTZ and the center of the olefin at bbpe is ~5 Å. If there are conformers in this case, the distance separating -$PTZ^{\bullet+}$ and $bbpe^{\bullet-}$ is the same for either.

The Lowest Excited State in [(4-Etpy)$(CO)_3$Re(μ-bbpe)-Re$(CO)_3$(4-Etpy)]$^{2+}$. The emission characteristics of [(4-Etpy)$(CO)_3$Re(μ-bbpe)Re$(CO)_3$(4-Etpy)]$^{2+}$ vary markedly with temperature in 4:1 (v:v) ethanol−methanol, Figure 2. There is a change in the characteristic, structured $\pi\pi^*$ emission at 77 K to a broad, featureless band at room temperature. Slight shifts occur in the spectrum through the glass to fluid transition at ~130−150 K. In fluid solution above 160 K, the emission intensity steadily decreases and the spectrum broadens. By 175 K there is nearly complete quenching of the structured emission. The emission profile was independent of excitation wavelength from 355 to 420 nm.

The change in behavior is consistent with a transition from a $\pi\pi^*$ emitter to a MLCT emitter. Related behavior has been observed by Schmehl et al. in [$(CH_3CN)(CO)_3$Re(dstyb)Re-$(CO)_3(CH_3CN)](PF_6)_2$ (dystb is 1,4-bis[2-(4′-methyl-2,2′-bipyridyl-4-yl)ethenyl]benzene) and in [(mstyb)Re$(CO)_3(CH_3CN)$]-(PF_6) (mstyb is 4-styryl-4′-2,2′-bipyridine), where based on

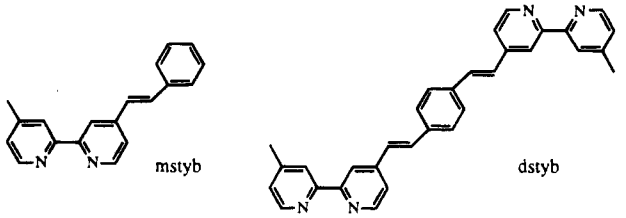

temperature dependent spectroscopic measurements, it has been concluded that a ligand-based $\pi\pi^*$ excited state lies lowest in energy. For the former, the $\pi\pi^*$ state remains the emitting state at room temperature.[22] For [Re(mstyb)$(CO)_3(CH_3CN)](PF_6)$, the room temperature emission spectrum is considerably broadened and blue-shifted similar to our observations for [(4-Etpy)-

(20) (a) Chen, P Y, Curry, M.; Meyer, T. J. *Inorg. Chem.* **1989**, *28*, 2271. (b) Tapolsky, G.; Duesing, R.; Meyer, T. J. *Inorg. Chem.* **1990**, *29*, 2285.

(21) (a) Chen, P Y; Duesing, R.; Tapolsky, G.; Meyer, T. J. *J. Am. Chem. Soc.* **1989**, *111*, 8305. (b) Chen, P Y; Duesing, R.; Meyer, T. J. *J. Phys. Chem.* **1991**, *95*, 5850.

(22) Shaw, J. R.; Schmehl, R. H. *J. Am. Chem. Soc.* **1991**, *113*, 389.

Scheme 2

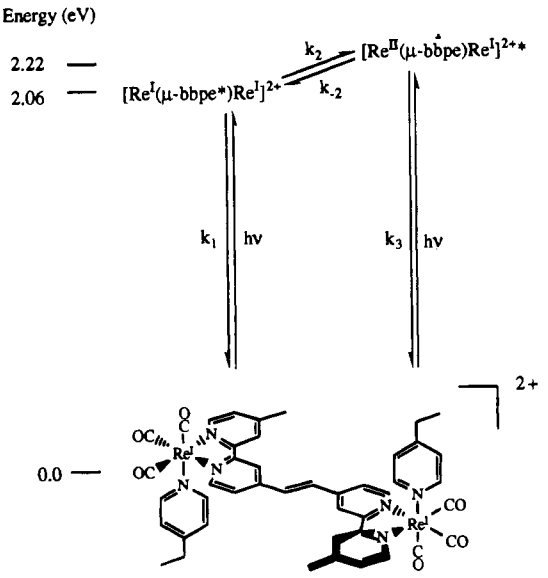

$(CO)_3Re(\mu\text{-bbpe})Re(CO)_3(4\text{-Etpy})]^{2+}$. Related observations were made earlier by Wrighton et al. and by Demas et al. in other complexes of Re^I where there are closely spaced excited states of different orbital origins.[23,24]

There is evidence in the transient absorption difference spectrum in Figure 5A for the coexistence of both MLCT and $\pi\pi^*$ excited states at room temperature. In this spectrum there are features for $bbpe^{\bullet-}$ at ~370 nm and ~520 nm and an additional intense feature at ~480 nm. This feature does not appear in the transient difference spectrum of $[(dmb)_2Ru^{III}(\mu\text{-}bbpe^{\bullet-})Ru^{II}(dmb)_2]^{4+}$ *. It may have its origin in the transition $T_1 \rightarrow T_2$ for the $\pi\pi^*$ excited state of bbpe. It is known in polyaromatic hydrocarbons that the energy of the $T_1 \rightarrow T_2$ transition is dependent on the number of electronically coupled aromatic units, e.g., λ_{max} is at 430 nm for anthracene and at 508 nm for tetracene.[25] The $T_1 \rightarrow T_2$, $\pi-\pi^*$ excited state in 2,2′-bipyridine on Rh(III) has been observed spectroscopically at 435 nm.[26]

It seems clear that the *lowest* excited state in $[(4\text{-Etpy})(CO)_3Re(\mu\text{-bbpe})Re(CO)_3(4\text{-Etpy})]^{2+}$ is $\pi\pi^*$(bbpe) with a closely lying MLCT state, Scheme 2. Excited state properties at or near room temperature are dominated by MLCT decay, given the relatively short excited state lifetime, Table 2.

It is possible to estimate the energies of the $\pi\pi^*$ and MLCT excited states from emission spectra by a Franck–Condon analysis of the spectral profiles by using a single mode approximation. This procedure has been described in detail elsewhere.[27,28] A comparison between experimental and calculated spectra is shown in Supplemental Figure 1. The energies of the excited states cited in Scheme 2 were estimated as follows:

(1) Spectral fitting of the room temperature emission spectrum, which is dominated by the MLCT state, gave E_0 (the $v^* = 0 \rightarrow v = 0$) energy gap in the single mode approximation) = 17 900 cm^{-1} and $\Delta\bar{\nu}_{0,1/2}$ (the full width at half-maximum) = 3000 cm^{-1}. The term $\Delta\bar{\nu}_{0,1/2}$ includes contributions from the solvent and low frequency modes treated classically.[27] The free energy of the excited state above the ground state, ΔG^0_{es}, was calculated from[28]

$$\Delta G^0_{es} = E_0 + [(\Delta\bar{\nu}_{0,1/2})^2/kT16(\ln 2)] = 18\,200\ cm^{-1}\ (2.26\ eV)$$

(2) For the $\pi\pi^*$ state, emission spectral fitting was performed at 160 K which is past the glass to fluid transition, with $\pi\pi^*$ still the dominant emitter. Spectral fitting gave E_0 = 16 600 cm^{-1} and $\Delta\bar{\nu}_{0,1/2}$ = 900 cm^{-1}, and from this, ΔG^0_{es} = 16 600 cm^{-1} (2.06 eV). This value is cited in Scheme 2. It assumes a negligible temperature dependence of ΔG^0_{es} for the $\pi-\pi^*$ state.

The energies derived from the spectral fits are only approximate but are consistent with the apparent ordering of the two states with both being sufficiently populated to be observed spectroscopically at room temperature.

The conclusion that the two states coexist is relevant to the observation of nonexponential emission decay kinetics over an extended temperature range, Supplemental Table 1. Although the kinetics for the two state case in Scheme 2 have been solved and are consistent with the observation of biexponential decay, it is not possible with our data to deconvolute the measured constants I_a, k_a, I_b, and k_b in eq 2 into the microscopic rate constants of Scheme 2.[29] However, there is qualitative information in these data about excited state dynamics. From the plot in Figure 4, the fraction of emission arising from the two components, F_A and F_B, is temperature dependent. The fraction associated with the faster decay F_B increases with temperature. This is qualitatively consistent with Scheme 2 with the relative fraction of the MLCT state increasing with temperature (and ΔH a positive quantity for the equilibrium between $\pi\pi^*$ and MLCT in Scheme 2). Because of its shorter decay time, the MLCT state dominates decay by 298 K. The kinetic quantities k_a and k_b at 298 K are considerably greater in magnitude (6.3 $\times 10^6\ s^{-1}$ and 0.46 $\times 10^6\ s^{-1}$) than is typically found for ligand-based, $\pi\pi^*$ excited states in related complexes.[22-24,30,31] Under these conditions $k_3 \gg k_1$ in Scheme 2, and excited state decay is dominated by the MLCT state. The nonexponentiality arises because the magnitudes of k_2, k_{-2}, and k_3 must be comparable. In this kinetic limit, the $\pi\pi^*$ state acts as a "reservoir" for the more rapidly decaying MLCT state.

An important inference to be drawn from this analysis and from the data presented by Schmehl et al., Wrighton et al., and Demas et al. is that $\pi\pi^* \leftrightarrow$ MLCT interconversions can be relatively slow. Although this is an interconversion between excited states, there is reason to believe that a reasonable kinetic barrier between states might exist. In terms of electronic configurations the transition is, $\pi\pi^*$ ($\pi^1 d\pi^6\pi^{*1}$) $\rightarrow$ MLCT ($\pi^2 d\pi^5\pi^{*1}$). Contributions to the barrier between states are expected from solvent repolarization because of the change in excited state dipole character between the $\pi\pi^*$ and MLCT excited states and, to a degree, from low frequency Re–N modes and ν(bpy) ring stretching modes.

(23) Sacksteader, L. A.; Lee, M.; Demas, J. N.; DeGraff, B. A. *J. Am. Chem. Soc.* **1993**, *115*, 8230.
(24) (a) Giordano, P. J.; Fredericks, S. M.; Wrighton, M. S.; Morse, D. L. *J. Am. Chem. Soc.* **1978**, *78*, 2257. (b) Fredericks, S. M.; Luong, J. C.; Wrighton, M. S. *J. Am. Chem. Soc.* **1979**, 7415.
(25) McGlynn, S. P.; Azumi, T.; Kinoshita, M. *Molecular Spectroscopy of The Triplet State* Prentice-Hall, Inc.: Englewood Cliffs, NJ 1969.
(26) Colombo, M. G.; Hauser, A., Guedel, H. U. *Inorg. Chem.* **1993**, *32*, 3088.
(27) (a) Lumpkin, R. S.; Worl, L. A.; Murtaza, Z.; Meyer, T. J.; Kober, E. M. Manuscript in preparation. (b) Kober, E. M.; Caspar, J. V.; Lumkin, R. S.; Meyer, T. J. *J. Phys. Chem.* **1986**, *90*, 3722. (c) Lumpkin, R. S. Ph.D. Dissertation, The University of North Carolina at Chapel Hill, 1986.
(28) Hupp, J. T.; Neyhart, G. A.; Meyer, T. J.; Kober, E. M. *J. Phys. Chem.* **1992**, *96*, 10820.
(29) Heitle, H.; Finckh, P.; Weeren, S.; Pöllinger, F.; Michel-Beyerle, M. E. *J. Phys. Chem.* **1989**, *93*, 5173.
(30) Shaw, J. R.; Webb, R. T.; Schmehl, R. H. *J. Am. Chem. Soc.* **1990**, *112*, 1117.
(31) Juris, A.; Campagna, S.; Bidd, I.; Lehn, J-M; Ziessel, R. *Inorg. Chem.* **1988**, *27*, 4007.

Initial Electron Transfer. The transient absorption and resonance Raman data demonstrate that intramolecular electron transfer occurs following $Re^I \rightarrow$ bbpe MLCT excitation of $[(py\text{-}PTZ)(CO)_3Re(\mu\text{-}bbpe)Re(CO)_3(py\text{-}PTZ)]^{2+}$ and $[(py\text{-}PTZ)(CO)_3Re^I(\mu\text{-}bbpe)Re^I(CO)_3(MQ^+)]^{3+}$. In the former case, the electronic structure is expected to be analogous to that in $[(4\text{-}Etpy)(CO)_3Re(\mu\text{-}bbpe)Re(CO)_3(4\text{-}Etpy]^{2+}$ and the state ordering in Scheme 2, or a similar one, should pertain. If this is so, and the magnitudes of the $\pi\pi^* \leftrightarrow$ MLCT dynamics are comparable, it follows that *both* MLCT and $\pi\pi^*$ excited states undergo reductive electron transfer to give the redox-separated state (eq 7). This follows from the conclusion in the previous section that k_2, k_{-2}, and k_3 are comparable in magnitude, the fact that the redox-separated state appears during the laser pulse (on a timescale short compared to the equilibration between states), and that emission (from MLCT) is completely quenched.

$$[(py\text{-}PTZ)(CO)_3Re^I(\mu\text{-}bbpe^*)Re^I(CO)_3(py\text{-}PTZ)]^{2+} \rightarrow [(py\text{-}PTZ^{\bullet+})(CO)_3Re^I(\mu\text{-}bbpe^{\bullet-})Re^I(CO)_3(py\text{-}PTZ)]^{2+} \quad (7a)$$

$$(\pi^1 d\pi^6\pi^{*1}-\pi^2{}_{PTZ}) \qquad (\pi^2 d\pi^6\pi^{*1}-\pi^1{}_{PTZ})$$

$$[(py\text{-}PTZ)(CO)_3Re^{II}(\mu\text{-}bbpe^{\bullet-})Re^I(CO)_3(py\text{-}PTZ)]^{2+} * \rightarrow [(py\text{-}PTZ^{\bullet+})(CO)_3Re^I(\mu\text{-}bbpe^{\bullet-})Re^I(CO)_3(py\text{-}PTZ)]^{2+} \quad (7b)$$

$$(\pi^2 d\pi^5\pi^{*1}-\pi^2{}_{PTZ}) \qquad (\pi^2 d\pi^6\pi^{*1}-\pi^1{}_{PTZ})$$

The complex $[(py\text{-}PTZ)(CO)_3Re(\mu\text{-}bbpe)Re(CO)_3(MQ^+)]^{3+}$ is electronically asymmetrical and the relative ordering of MLCT and $\pi\pi^*$(bbpe) states is not clear. In any case, whether $\pi\pi^*$ or MLCT is lowest, electron transfer occurs during the laser pulse to give the redox-separated state, as shown in Scheme 1.

Acknowledgement is made to the National Science Foundation for financial Support under Grant No. CHE-8806664.

Supplementary Material Available: The kinetic data for the temperature dependence of emission lifetimes in 4:1 (v:v) ethanol–methanol for $[4\text{-}Etpy)(CO)_3Re(\mu\text{-}bbpe)Re(CO)_3(4\text{-}Etpy)](PF_6)_2$ are provided for the temperature range 77.0–295.0 K in Supplemental Table 1. Franck–Condon anaylses of emission spectra of $[4\text{-}Etpy)(CO)_3Re(\mu\text{-}bbpe)Re(CO)_3(4\text{-}Etpy)](PF_6)_2$ at 77 K and 298 K in 4:1 ethanol–methanol and procedural information about the fitting are presented in Supplemental Figure 1 and text (5 pages). Ordering information is given on any current masthead page.

IC940375J